ISSN: 2633-4828 Vol. 8 No.2, June, 2026

International Journal of Applied Engineering & Technology

BIAXAIL STRESS-STRAIN RELATIONS OF PLAIN CONCRETE USING EQUIVALENT UNIAXIAL STRAIN

Kallakury Srinivas [1*], Dr. P. Subba Rao[2]

[1*] Research Scholar, Civil Engineering Dept., J N T U K, Kakinada.
[2] Professor, Civil Engineering Dept., J N T U K, Kakinada
Corresponding Author: E-mail: [1]ksrinivasrb@gmail.com, [2]srpalivela@jntucek.ac.in
Received: 15 May 2026, Revised: 18 June 2026, Acceptance: 19 July 2026, Publication: 25 July 2026

Abstract
In this work, new equations for peak stress-strain relations for the principal stress ratio, α, from 0.0001 to 1 for plain normal concrete under biaxial compression are presented. $\boldsymbol{\alpha} < 0.0001$ *is treated as uniaxial compression case. At* $\alpha = 0.223$ *, the principal strain in 1-direction changes its sign from tensile state to compressive state. A methodology for duplicating the uniaxial curves from biaxial stress-strain relations is presented. New equations for biaxial compression are proposed. The equations are framed based on the work of Kupfer and Gerstle and the nonlinear biaxial stress-strain law proposed by Darwin and Pecknold. The biaxial stress-strain curves can easily be constructed based on the equations, in the biaxial compression state, along with appropriate equations for biaxial tension, tension-compression, and compression-tension for any principal stress ratio. An effective Poisson's ratio of 0.2 is used for biaxial tension and biaxial compression. For T-C material routine, Poisson's ratio based on the strain ratio proposed by Elwi and Murray is utilized. To duplicate the curves under C-T a different methodology is employed. The study discusses the biaxial behaviour of normal concrete up to peak stress using Saenz's equation based on an incremental-iterative hypoelastic model. Nevertheless, the methodology can be extended to high-strength and high-performance concretes with an incremental secant formulation or a total secant formulation based on the elastic properties of concrete. These equations are utilized in the design of the bridge slabs and the beams using MATLAB.*

Keywords: *Biaxial response, stress-strain relations, hypo elastic, concrete, incremental-iterative, tangent stiffness, stress ratio, nonlinear, equivalent uniaxial strain.*

1. INTRODUCTION

The study of Reinforced Concrete structures requires knowledge of materials, their behavior and their interaction to act as a composite under the influence of external loads. Structural analysis integrates material mechanics to achieve resource optimization without compromising structural safety. The introduction of new materials in the construction industry has reinforced the necessity to study their properties and to explore their full potential. The development of numerical methods such as finite element analysis has enabled the assessment of material's state at any given instant. Structures must be analysed by considering the interaction of internal and embedded elements to achieve realistic and optimum design. The analysis of reinforced concrete elements is complex in nature due to non-linear stress – strain relations, the yielding of steel, cracking of concrete and time dependent effects like creep and shrinkage [1]. Slabs, thin shells, and shear walls exhibit inherent biaxial behaviour; therefore, they must be modelled under a biaxial stress state [2]. Experimental studies [3] have facilitated the simulation of the biaxial response of reinforced concrete structures under representative loading conditions [4-6].

Darwin and Pecknold proposed the equivalent uniaxial strain concept to map biaxial stress-strain behaviour of concrete to uniaxial curves, by separating Poisson's effect, through the principal stress ratio,α [2]. In this method, the strain increment is assessed from the principal stress increment in that direction and the corresponding tangent stiffness [7]. They employed Saenz's equation to model the biaxial stress-strain curves of concrete under compression utilizing the concept of equivalent uniaxial strain,ϵ_{iu}, which they devised. The variables in the Saenz's equation are $E_0, \epsilon_{iu}, E_s, \epsilon_{ic}$, where, E_0 is initial tangent modulus can be determined from the experiments or based on the equations given in the codes, E_s is the secant modulus at the point of peak stress and is the ratio of peak stress,σ_{ic} to peak strain,ϵ_{ic}. Using these variables, the corresponding stress in the principal direction and the tangent modulus can be evaluated. The only limitation of using this equation is determining the parameters $\sigma_{ic}$and ϵ_{ic}. They used the experimental results of Kupfer et al., Liu et al. and Nelissen [4-6] to derive the stress- strain relations of concrete for different principal stress ratios under biaxial compression, biaxial tension, tension-compression and compression- tension.

This approach was actively utilised in the works of Rajagopal [8], Bashur [9], Elwi and Murray [10], Balan [1], He et. al. [11], Cerioni and Donida [12], Wang [13], Ng[14], Bono et al. [15], and Kwan et al. [16].

Ferriera et al. [17] in their study employed equivalent uniaxial strain concept and they have considered the lateral effects on concrete by calculating the equivalent uniaxial strains given by DIANA (2016).

In the present work, an incremental-iterative approach based on a tangent stiffness formulation has been adopted to study the biaxial response of concrete in both the pre-peak and post-peak regimes. As bridge structures are subjected to complex and repeated loading histories, a tangential stress–strain relationship is essential to accurately model progressive stiffness degradation and path-dependent material behaviour, following the orthotropic model proposed by Darwin and Pecknold [2]. Based on strain-displacement relations, the axial displacements are C^0-continuous elements whereas transverse displacement and rotations are C^1-continuous, and accordingly, Lagrange interpolation functions and Hermite interpolation functions are incorporated into the analysis [18-19]. A 4-node, 24-degree-of-freedom (DOF) rectangular plate bending element is utilized, adopting the Kirchhoff hypothesis and integrating geometric nonlinearities through a layered formulation. In order to study the stress-strain curve of concrete completely, the displacement control method is applied as a nonlinear solution strategy [20-21]. The study focuses on the optimum design of reinforced concrete (RC) T-beam girder bridges utilizing nonlinear finite element analysis (NLFEA). The Indian Roads Congress (IRC) [22-23] is currently revising the Standard Bridge Drawings to transition from the Working Stress Method (WSM) to the Limit State Method (LSM); therefore, the present study is particularly timely. In this respect, for updating the stresses and tangent moduli, the peak stress and peak strain corresponding to the biaxial principal stress ratio are calculated to replicate the biaxial philosophy into uniaxial modelling. In the present paper, the pre-peak material concepts based on equivalent uniaxial strain as per an equation proposed by Saenz for ascending portion of the stress- strain curve are described in Section 2.

2. Material Modelling

2.1. Concrete pre- peak modelling

Concrete under the biaxial stress state is characterized by four distinct material routines: (a) the Biaxial Tension (T–T) state; (b) the Tension–Compression (T–C) state; (c) the Compression–Tension (C–T) state; and (d) the Biaxial Compression (C–C) state [4]. To formulate a numerical model capable of simulating these experimental states, equivalent uniaxial strain concept introduced by Darwin and Pecknold is employed [2].

Eq. (1) defines the orthotropic incremental stress–strain relationship referred to the current principal material axes and is adopted in the present study [2]. Here, $\{d\sigma_1, d\sigma_2, d\tau_{12}\}^T$ and $\{d\epsilon_1, d\epsilon_2, d\gamma_{12}\}^T$ represent incremental stresses and incremental strains respectively in the principal material directions.

$$\begin{Bmatrix} d\sigma_1 \\ d\sigma_2 \\ d\tau_{12} \end{Bmatrix} = \frac{1}{1-\nu^2}\begin{bmatrix} E_1 & \nu\sqrt{E_1E_2} & 0 \\ \nu\sqrt{E_1E_2} & E_2 & 0 \\ 0 & 0 & \dfrac{E_1+E_2-2\nu\sqrt{E_1E_2}}{4} \end{bmatrix}\begin{Bmatrix} d\epsilon_1 \\ d\epsilon_2 \\ d\gamma_{12} \end{Bmatrix} \tag{1}$$

$$\{\sigma_c\} = [D_c]\{\epsilon_c\} \tag{2}$$

In Eq. (1), $E_1$and E_2 are the tangent moduli referred to material axes (1, 2), while ν is effective Poisson's ratio. $E_1$and E_2 are calculated from the stress-strain relationship suggested by Saenz [2] for compressive loading. D_c is stress-strain matrix in material directions. The equivalent uniaxial strain concept is utilized in Eq. (3) , Saenz's equation is adopted for pre-peak portion of the stress- strain curve.

$$\sigma_i = \frac{(\epsilon_{iu}E_0)}{1+\left(\frac{E_0}{E_s}-2\right)\left(\frac{\epsilon_{iu}}{\epsilon_{ic}}\right)+\left(\frac{\epsilon_{iu}}{\epsilon_{ic}}\right)^2} \tag{3}$$

The tangent modulus in i-th direction, E_i can be calculated by differentiating Eq. (4) with respect to ϵ_{iu}

$$E_i = \frac{E_0\left(1-\left(\frac{\epsilon_{iu}}{\epsilon_{ic}}\right)^2\right)}{\left(1+\left(\frac{E_0}{E_s}-2\right)\left(\frac{\epsilon_{iu}}{\epsilon_{ic}}\right)+\left(\frac{\epsilon_{iu}}{\epsilon_{ic}}\right)^2\right)^2} \tag{4}$$

Wherein , σ_i is stress in i th direction in material axes; $\epsilon_{iu}$is equivalent uniaxial strain at i-th direction; E_0 initial tangent modulus;$E_s = \frac{\sigma_{ic}}{\epsilon_{ic}}$ =secant modulus at the point of maximum compressive stress, σ_{ic}; and ϵ_{ic}= equivalent uniaxial strain at the point of maximum compressive stress.

E_0 can be determined from uniaxial compression test or calculated as suggested in the standards. σ_{ic} and ϵ_{ic} depend on principal stress ratio,$\alpha = \left(\frac{\sigma_1}{\sigma_2}\right)$,where $\sigma_1 \geq \sigma_2$. σ_{ic} , can be assessed from biaxial strength envelope proposed by Kupfer and Gerstle [2]. The equivalent uniaxial strain ϵ_{iu} essentially removes the Poisson's effect, whereas strengthening and ductility increase effects are incorporated in σ_{ic} and ϵ_{ic} respectively [24,7]. That is, the effect of principal stress ratio on stress – strain response is primarily contained in σ_{ic} and ϵ_{ic} and the effect of Poisson's ratio is contained in ϵ_{iu}[24,7].

$$\epsilon_{iu} = \sum_{\substack{\text{load} \\ \text{increments} \\ \text{or} \\ \text{displacement} \\ \text{increments}}} \frac{\Delta\sigma_i}{E_i} \tag{5}$$

Where $\Delta\sigma_i$ = incremental change in principal stress σ_i; E_i = varying tangent stiffness corresponding for load or displacement increment corresponding to $\Delta\sigma_i$.

For brevity, only constitutive equations and simulation graphs are presented.

(A) Biaxial Tension (T–T) state ($1 < \alpha < \infty$)

Two concepts are described as below based on the works of Kupfer and Gerstle [4], Kupfer et al. [25], Darwin and Pecknold [2], Ramaswamy [8], He et al. [11], Wang [26], Ganaba [27] and Ng [14].

(i). The concrete response under biaxial tension state is assumed to be linearly elastic up to f_t , uniaxial tensile strength of concrete, and thus tangent modulus E_i is equal to initial tangent modulus until cracking initiates [2,25,8,27,11,26].

$$\sigma_{ic} = f_t \tag{6}$$
$$E_i = E_0 \tag{7}$$
$$\epsilon_i = \frac{\sigma_{ic}}{E_i} \tag{8}$$

i-th direction can be 1 or 2 employed with appropriate equivalent uniaxial strain.

(ii). Ng [14] in his work utilized the experimental results of Guo and Zhang and assumed that peak tensile strain under uniaxial tension is 20% greater than f_t/E_0. The equations [14] for computation of stresses and Tangent moduli are given below

$$\sigma_i = f_t\left[1.2\left(\frac{\epsilon_{iu}}{\epsilon_{ic}}\right) - 0.2\left(\frac{\epsilon_{iu}}{\epsilon_{1c}}\right)^6\right] \tag{9}$$
$$\epsilon_{1c} = \epsilon_{2c} = \frac{1.2 f_t}{E_0} \tag{10}$$
$$E_i = \left(\frac{1.2 f_t}{e_{2c}}\right)\left(1 - \left(\frac{\epsilon_{2u}}{\epsilon_{2c}}\right)^5\right) \tag{11}$$

These two methods are mapped onto the experimental curves and are shown in Fig. 2.1 and Fig 2.2

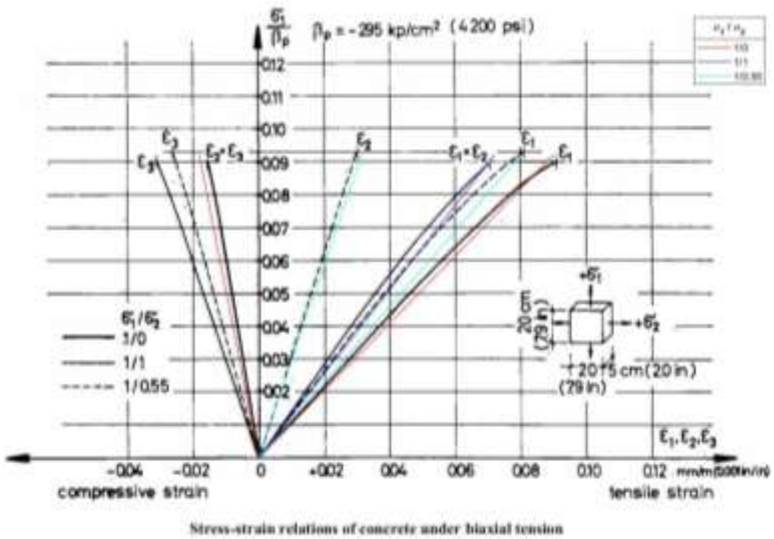

Fig 2. 1. Stress-strain response of concrete under biaxial tension using linearly elastic relations

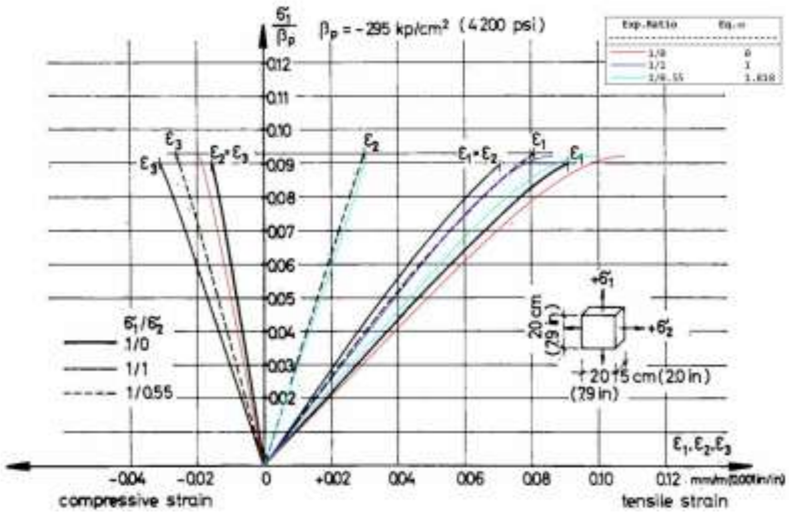
Fig 2.2. Stress-strain response of concrete under biaxial tension using the Ng formulation

An effective Poisson's ratio of 0.2 is adopted for this zone.

(B) Biaxial Tension- Compression (T–C) region ($-\infty < \alpha \leq -0.0245$)

The tension–compression routine is subdivided into tension–compression (T-C) and compression- tension (C-T) regions, depending on the failure mode associated with α. This region is represented by a linear reduction of tensile stress with increasing compressive stress followed by curved part up to f_c [14]. In the present study, the ratio of uniaxial tensile strength of concrete to uniaxial compressive strength of concrete is assumed to be -0.1. Based on this strength ratio, at a principal stress ratio of α = -0.0245, calculated by equating the compressive strengths of the linear and curved zones, the routine transitions from a linear T–C region to a parabolic C–T region [28]. It was reported by Kupfer et al. as -1/15 and the uniaxial strength ratio corresponding to their work is $= -0.09$ [29], but in the present work it is assumed as -0.1. To simulate the work of the Kupfer et al., a ratio of -0.0221 is utilized for distinguishing these two routines. The generic equation for calculating the limits based on the uniaxial strength ratio is defined in Eq. (17). In this region, a crack is assumed to occur in a plane normal to the direction of offending maximum principal stress, when tensile stress or tensile strain exceeds the limiting value, namely the limiting tensile strength, f_t or the limiting tensile strain,ϵ_t [30]. The parameters $\sigma_1, and\ E_1$ in this region are calculated using the methods described for biaxial tension by replacing f_t in Eqs. (9), (10) and (11) with σ_{1c} determined by Eq. (13). The stress-strain relations in the second direction are computed based on Eqs. (14) to (17) defined for both zones. The principal stresses and tangent moduli for 2-direction in the T–C zone as well as 1-and 2-directions in the C–T region are determined based on Saenz's equation presented in Eq. (3). In the T-C routine, the varying Poisson's ratio concept of Elwi and Murray [10] is employed, whereas for the C-T region an effective Poisson's ratio of 0.2 is used. The calculation of variables for determining σ_1, E_1 $, \sigma_2\ and\ E_2$ are presented below. ϵ_{1c} in the C-T region, for application of Saenz' equation, is calculated by interpolation between peak tensile strains at uniaxial tensile state, $\epsilon_{t,}$ and that at uniaxial compression state,$\epsilon_{tc.}$, and then divided with $(1 - \nu/\alpha)$ .The peak compressive strain ϵ_{2c} adopted in the work, defined in Eqs. (15) and (16), is originally developed by the authors to calculate ϵ_{1c} in 1-direction under biaxial compression.

$$\alpha^2(3.65 - s) + \alpha(1 + .92s) - 0.2s = 0 \tag{12}$$

where $s = \frac{f_t}{f_c}, \ and \ \ f_c \ denotes \ the \ uniaxial \ compressive \ strength \ of \ concrete.$

(1) **Biaxial Tension-Compression (T-C) zone ($-\infty \ < \ \boldsymbol{\alpha} \leq -\mathbf{0.0245}$)**

$$\frac{\sigma_{1c}}{fc} = 1 - 0.8\frac{\sigma_{2c}}{f_c} \tag{13}$$

$$\sigma_{2c} = \frac{\sigma_{1c}}{\alpha}, \tag{14}$$

a) up to $\sigma_{2c} = 0.652f_c$

$$\epsilon_{2c} = 1.104\epsilon_c\left[\frac{\sigma_{2c}}{fc}\right] \tag{15}$$

b) $0.652f_c \leq \sigma_{2c} \leq f_c$

$$\epsilon_{2c} = \epsilon_c\left[0.805\frac{\sigma_{2c}}{fc} + 0.195\right] \tag{16}$$

Where ϵ_c is the uniaxial compressive strain of concrete

$$v_i = v_0\left[1.0 + 1.3763(\frac{\epsilon_{iu}}{\epsilon_{ic}}) - 5.36\left(\frac{\epsilon_{iu}}{\epsilon_{ic}}\right)^2 + 8.586\left(\frac{\epsilon_{iu}}{\epsilon_{ic}}\right)^3\right] \ngtr 0.5 \tag{17}$$

where v_i = Poisson's ratio in i-th direction under consideration, ν_0 initial Poisson's ratio and is equal to 0.2.

$$\nu = \sqrt{\nu_1\nu_2} \tag{18}$$

wherein, ν = Effective Poisson's ratio.

(C) Biaxial Compression-Tension (C–T) region ($-\mathbf{0.0245} \leq \ \boldsymbol{\alpha} < \ \mathbf{0}$)

In this region, compressive crushing or combined crushing and splitting failure takes place [26]. A crushing type of fracture can be observed under the influence of multi axial compressive states [30]. The peak compressive strengths are calculated by using the Eq. (19) and (20) . An effective Poisson's ratio of 0.2 is considered.

$$\sigma_{2c} = \frac{1 + 3.65\alpha}{(1 + \alpha)^2}f_c \tag{19}$$

$$\sigma_{1c} = \alpha\sigma_{2c} \tag{20}$$

$$\epsilon_{1c} = \epsilon_t + \left[\frac{\epsilon_{tc} - \epsilon_t}{f_t}(f_t - \sigma_{1c})\right] \tag{21}$$

where ϵ_t is the uniaxial tensile strain and ϵ_{tc} is the maximum tensile strain of concrete under uniaxial compression?

The peak compressive strains, $\epsilon_{1c} \ and \ \epsilon_{2c}$ are determined based on Eq. (16) and Eq. (21).

The numerical modelling is superimposed on the experimental curves [15] and is shown in Fig. 2.3, Fig 2.4. and Fig 2.5.

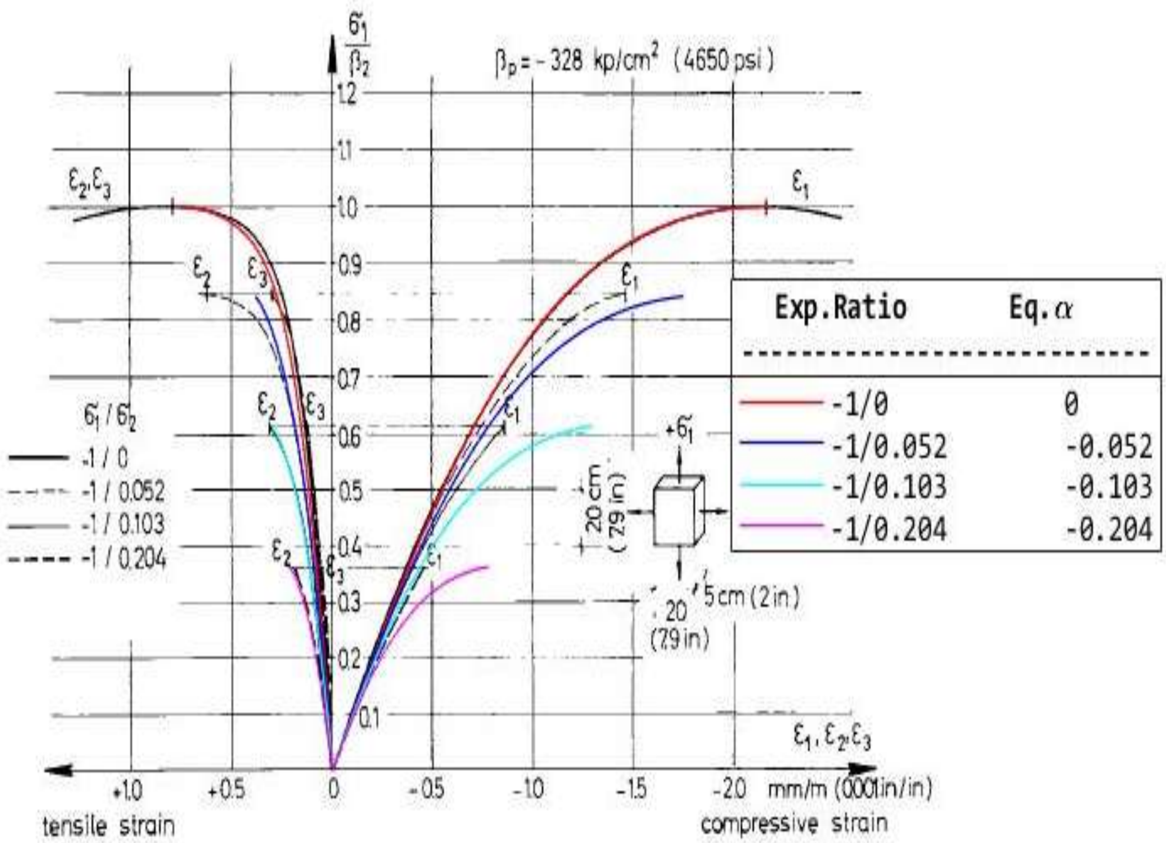

Fig 2.3. Stress-strain response of concrete under biaxial tension-compression using the linear model in the 1-direction and proposed equations in the 2-direction

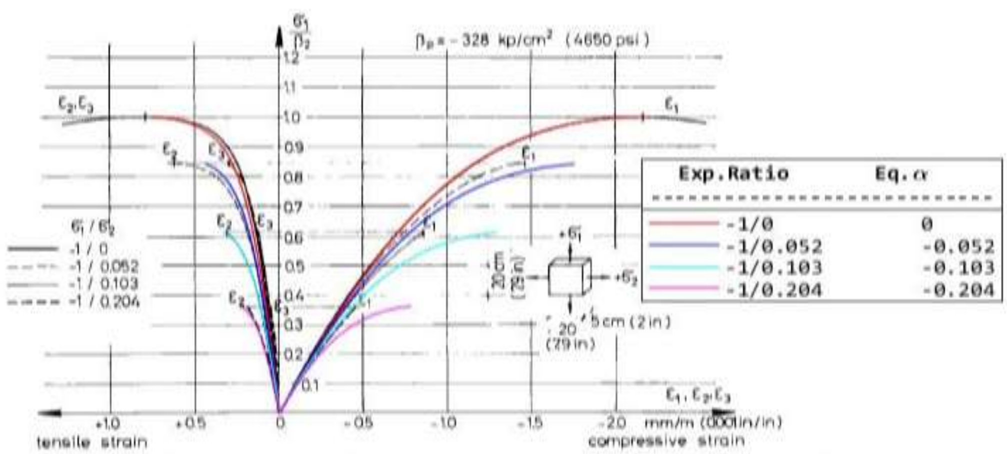

Fig 2. 4. Stress-strain response of concrete under biaxial tension-compression using the Ng formulation in the 1-direction and the proposed equations in the 2-direction

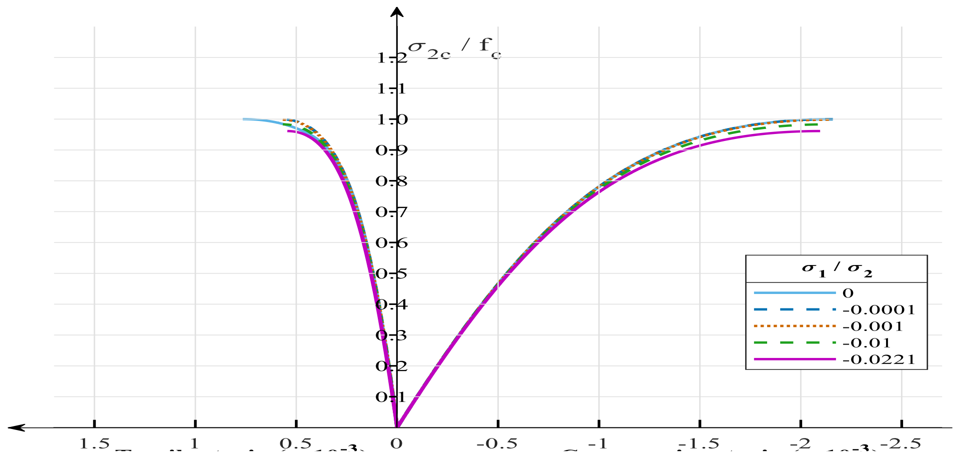

Fig. 2. 5. Stress-strain response of concrete under biaxial tension-compression using the proposed equations for different principal stress ratios

(D) Biaxial compression (C-C) region ($0 \leq \alpha \leq 1$)

In this routine, concrete fails due to crushing. Peak stresses,σ_i and peak strain ϵ_{2c} are calculated in accordance with the procedure suggested by Darwin and Pecknold [2]. The equations for ϵ_{1c} are formulated using an iterative curve-fitting method and are presented in Eqs.(15) and (16). The principal strain,ϵ_1 is tensile under uniaxial compression and gradually transitions into the compressive strain [31]. This phenomenon is observed at $\alpha \approx 0.223$,and the governing equations for ϵ_{1c} are defined in Eqs.(15) and (16).

$$\sigma_{2c} = \frac{1 + 3.65\alpha}{(1+\alpha)^2} f_c \tag{22}$$

$$\sigma_{1c} = \alpha \sigma_{2c} \tag{23}$$

$$\epsilon_{2c} =. \epsilon_c \left[R \frac{\sigma_{2c}}{fc} + (R-1) \right] where\ R = 2.91 \tag{24}$$

The equations for the peak strains according to Darwin and Pecknold [2] for the two directions are defined in Eqs. (25) and (26).

$$\epsilon_{1c} = \epsilon_c \left[-1.6 \left(\frac{\sigma_{1c}}{f_c} \right)^3 + 2.25 \left(\frac{\sigma_{1c}}{f_c} \right)^2 + 0.35 \left(\frac{\sigma_{1c}}{f_c} \right) \right] \tag{25}$$

$$\epsilon_{2c} = \epsilon_c \left[3 \left(\frac{\sigma_{2c}}{f_c} \right) - 2 \right] \tag{26}$$

The numerical curves are superimposed on the experimental curves [15] and are shown in Fig. 2.6, Fig 2.7 and Fig 2.8.

All the concepts discussed in this section are validated against the experimental curves developed by Kupfer et al., and the observations are detailed in Section (3).

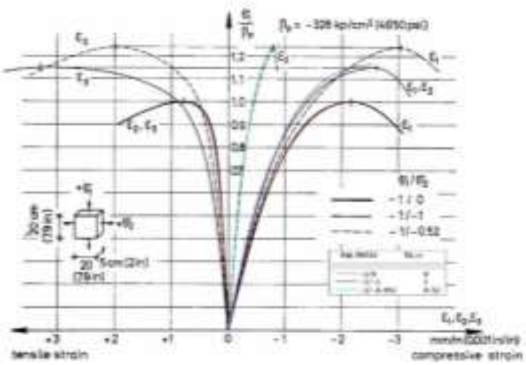

Fig 2. 6. Stress-strain response of concrete under biaxial compression using Darwin and Pecknold equations

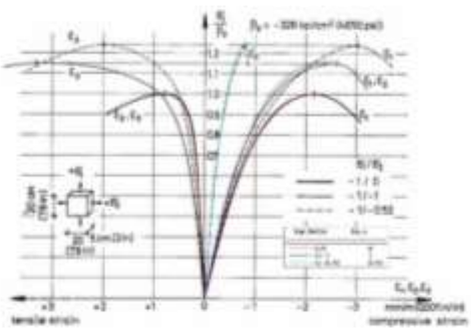

Fig 2. 7. Stress-strain response of concrete under biaxial compression using the proposed equations

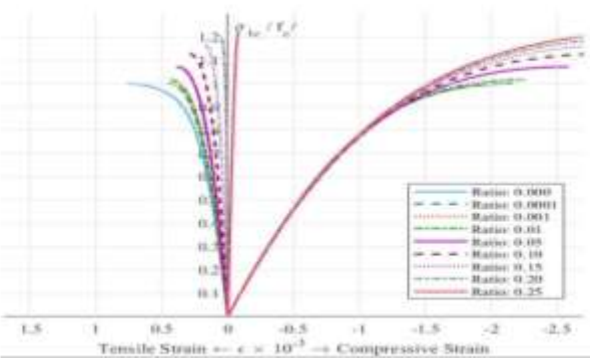

Fig 2.8. Family of biaxial Compression curves for different principal stress ratios using the proposed equations

3. Parametric study

The comparative parametric study deduced from Figs. 1 to 4 are detailed in the following tables. All the calculations, iterations are done using MATLAB 2021b. The experimental results, utilised for validating the numerical computations, are extracted using ORIGIN 2018.

(A) Biaxial Tension (T–T) state $(1 \leq \alpha < \infty)$

Table 1 Comparison of experimental and predicted principal strains under biaxial tension.

S. No.	Exp. notation	Principal stress ratio, α	Kupfer et al.[15]		Linear relations -Fig.1				Ng formulation-Fig.2			
			$\epsilon_{1c}(10^{-}$	$\epsilon_{2c}(10^{-}$	$\epsilon_{1c}(10^{-}$	% Var.	$\epsilon_{2c}(10^{-}$	% Var.	$\epsilon_{1c}(10^{-}$	% Var.	$\epsilon_{2c}(10^{-}$	% Var.
1	1/0	1.00	0.0911	-0.0155	0.0898	-1.43	-0.0179	15.48	0.1077	18.22	-0.0193	24.52
2	1/1	1.00	0.0705	0.0705	0.0719	1.99	0.0719	1.99	0.0861	22.13	0.0861	22.13
3	1/0.55	1.818	0.0808	0.0302	0.0799	-1.11	0.0314	3.97	0.1001	23.89	0.0301	-0.33

B.1) Biaxial Tension - Compression (T–C) state $(-\infty < \alpha < -0.0221)$

Table 2 Comparison of experimental and predicted principal strains under biaxial tension-compression.

S. No	Exp. notation	Principal stress ratio, α	Kupfer et al.[15]		Linearly elastic relations-Fig.3				Ng formulation-Fig.4			
			$\epsilon_{1c}(10^{-}$	$\epsilon_{2c}(10^{-}$	$\epsilon_{1c}(10^{-}$	% Var.	$\epsilon_{2c}(10^{-03}$	% Var.	$\epsilon_{1c}(10^{-}$	% Var.	$\epsilon_{2c}(10^{-}$	% Var.
1	-1/0	-0	0.7846	-2.160	0.7653*	-2.46	-2.16*	0.00	...	...	...	...
2	-1/0.052	-0.052	0.6117	-1.4613	0.3847	-37.11	-1.7299	18.38	0.4387	-28.28	-1.7355	18.76
3	-1/0.103	-0.103	0.3064	-0.8635	0.3034	-0.98	-1.2812	48.37	0.3368	9.92	-1.2789	48.11
4	-1/0.204	-0.204	0.1850	-0.4704	0.2151	16.27	-0.7692	63.52	0.2405	30.00	-0.7732	64.37

B.2) Biaxial Compression - Tension (C–T) state $(-.0221 \le \alpha \le 0)$

Table 3 Comparison of experimental and predicted principal strains under biaxial tension-compression.

S. No.	Principal stress ratio, α	Linearly elastic relations		Ng formulation		Eq.3 and proposed equationns-Fig.5	
		$\epsilon_{1c}(10^{-03})$	$\epsilon_{2c}(10^{-03})$	$\epsilon_{1c}(10^{-03})$	$\epsilon_{2c}(10^{-03})$	$\epsilon_{1c}(10^{-03})$	$\epsilon_{2c}(10^{-03})$
1.	0	0.4278	-2.1542	0.5176	-2.1620	0.7653*	-2.16*
2	-0.0001	0.4280	--2.1574	0.5167	-2.1574	0.5771	-2.1574
3	--0.001	0.4281	-2.1516	0.5162	-2.1516	0.5755	-2.1517
4	-0.01	0.4307	-2.1283	0.5192	-2.1292	0.5665	-2.1295
5	-0.0221	0.4332	-2.0941	0.5219	-2.0960	0.5443	-2.0960

C) Biaxial Compression - Compression (C–C) state ($0 < \alpha \leq 1$)

Table 3 Comparison of experimental and predicted principal strains under biaxial compression.

S. No.	Exp. notation	Principal stress ratio, α	Kupfer et al.		Darwin & Pecknold-Fig.6				Proposed equations -Fig.7			
			$\epsilon_{1c}(10^{-}$	$\epsilon_{2c}(10^{-}$	$\epsilon_{1c}(10^{-}$	% Var.	$\epsilon_{2c} * 10^{-03}$	% Var.	$\epsilon_{1c}(10^{-}$	% Var.	$\epsilon_{2c} * 10^{-03}$	% Var.
1	-1/0	0	7.8460	-2.1600	...	...	...	...	0.7653*	-2.46	-2.16*	0.00
2	-1/-1	1	-2.600	-2.6000	-2.5570	-1.65	-2.5570	-1.65	-2.5312	-2.65	-2.5312	-2.65
3	-1/-0.52	0.52	-0.8053	-3.0000	-0.9130	13.37	-3.4331	14.44	-0.8814	9.45	-3.3916	13.05

* Saenz's philosophy is applied for both the principal directions in compression– compression state, incorporated proposed equations with varying Poisson's ratio. $\alpha \leq -1 * 10^{4}$ is assumed as uniaxial compression case.

Note. σ_{1c} =peak compressive strength; f_c = uniaxial compressive strength; ϵ_{1c} *and* ϵ_{2c} = principal strains; % Var. = percentage variation between experimental, Kupfer et al. and computed values.

The observations drawn from these tables are presented below, which forms the basis for the structural analysis and design of the bridge deck and girders.

1. The stresses in concrete under biaxial tension are evaluated based on the two methods described under the biaxial tension. The peak tensile strains obtained by linearly elastic relations are varying from the experimental curves [3] in the range of -1.11% to 1.99% in the 1-direction and 1.99% to 15.48% in the 2-direction, whereas in the Ng formulation, they range from 18.22% to 23.89% and -0.22% to 24.52% respectively. From the curves, it can be observed that the Ng formulation traces the experimental path. Tasuji et al. [32], in their work presented the peak tensile stain under biaxial tension as 0.00015. The Ng formulation is employed in the present work, although the results are higher than the experimental observations of Kupfer et al. [6], in order to balance the conventional concepts with rational methods.
2. At the transition, from T-C state to C-T state, the methodology adopted by Ng [14] matches Saenz's model within a -4.12% range, compared to the linear conventional stress-strain relations which underestimates the strains by 20.41%.
3. The varying Poisson's ratio suggested by Elwi and Murray [10] is adopted for biaxial tension – compression routine and yielded good results.
4. Under the biaxial T-C state, the strain calculations based on Ng [14] and linear relations are lower than experimental results [2] by 12-38% on the tension side, and higher by 18-63% on the compression side; however, the path of the numerical curve follows the experimental curve and the higher computed strains on the compression side are due to imposing Saenz's assumptions into the proposed equations. This pattern is also observed in the work of He [28] where he validated his proposed equations against the work of Tasuji et al. In the C-T state, the proposed equations show a gradual increase with an increase in negative ratios and stabilize around $\alpha \leq -1 \times 10^{-4}$ and hence this ratio is considered to be the threshold limit for assuming concrete to be in a uniaxial compression stress state.
5. Under the biaxial C-C state, the experimental results, benchmark values [6] and proposed equations are in the close agreement by -3% to 14%.

6. A family of curves for different principal stress ratios is presented in Fig.(8), and it is observed that the principal strain in direction 1 changes from a tensile to a compressive nature at $\alpha \approx 0.223$.It is observed by Guo [31] that the strain in the 1-direction varies almost linearly ; it is tensile under the uniaxial state and gradually transits into a compressive nature. For brevity, the values are not shown in tabular form.

4. Conclusions

The following conclusions are deduced from the observations:

1. The proposed equations for biaxial compression in the principal direction 1 are verified with experimental results and found to be in good agreement under tension-compression, compression-tension and biaxial compression.

2. The equations are found to be stable, demonstrating no numerical instabilities, and stabilize at the principal stress ratios of -1×10^{-4} *and* 1×10^{-4}. The proposed equations are robust, sound and make it easy to assess the nonlinear behavior and response of plain concrete across all four biaxial stress states under different principal stress ratios,α.

References:

1. Balan TA, Filippou FC, Popov EP. Constitutive model for 3D cyclic analysis of concrete structures. J Eng Mech. 1997;123(2):143-153.
2. Darwin D, Pecknold D.A. Nonlinear biaxial stress-strain law for concrete. J Eng Mech Div. 1977;103(2):229-241.
3. Kupfer, H. B., and Gerstle, K. H. (1973). "Behaviour of concrete under biaxial stresses." J. Eng. Mech. Div., 99(4), 853–866
4. Liu TCY, Nilson AH, Slate FO. Biaxial stress-strain relations for concrete. J Struct Div. 1972;98(5):1025-1034.
5. Nelissen, L. J. M. (1972). "Biaxial testing of normal concrete." HERON, 18(1), 1–90.
6. Kupfer, H. B., and Gerstle, K. H. (1973). "Behaviour of concrete under biaxial stresses." J. Eng. Mech. Div., 99(4), 853–866.
7. Wai-Fah Chen, Plasticity in Reinforced concrete, J. Ross publishing, Cengage learning, Third Indian reprint, 2014.
8. Rajagopal, K.R. Nonlinear analysis o reinforced concrete beams, beam-columns and slabs by finite elements, Ph.D. thesis, Iowa State University, 1976
9. F. K. Bashur and D. Darwin, "Nonlinear model for reinforced concrete slabs," University of Kansas Center for Research, Lawrence, KS, USA, Tech. Rep. NSF-ENG76-09444, Dec. 1976.
10. Elwi, A. A., & Murray, D. W. (1979). A 3D hypo elastic concrete constitutive relationship. Journal of the Engineering Mechanics Division, 105(4), 623–641.
11. He, W., Wu, Y.-F., Liew, K. M., & Wu, Z. (2006). A 2D total strain based constitutive model for predicting the behaviors of concrete structures. International Journal of Engineering Science, 44(18-19), 1280–1303. doi.org
12. Cerioni, R., & Donida, G. (1994). A finite element model for the nonlinear analysis of reinforced and prestressed masonry walls. Computers & Structures, 53(5), 1047–1061. doi.org
13. Wang, Wenyuan, Nonlinear finite element analysis of reinforced concrete flat plate floors, Ph. D Thesis, Nanyang Technological University, Singapore,2007.
14. Ng Pui Lam, constitutive modelling and finite element analysis of reinforced concrete structures, Ph.D. Thesis, The University of Hong Kong, 2007.
15. Bono, G. F. F., Campos Filho, A., & Pacheco, A. (2011). A 3D finite element model for reinforced concrete structures analysis. Revista IBRACON de Estruturas e Materiais, 4(4), 524-541.

16. Kwan, A. K. H., Z. M. Wang, and H. C. Chan. "Mesoscopic Study of Concrete II: Nonlinear Finite Element Analysis." Computers & Structures, vol. 70, no. 5, 1999, pp. 545-556.
17. Ferreira, C., Sousa, C., Azenha, M., Schlicke, D., & Faria, R. (2025). A Pointwise Model Based on a Total Strain Approach to Simulate Long-term Concrete Behaviour. Journal of Advanced Concrete Technology, 23(5), 257–272. https://doi.org/10.3151/jact.23.257
18. Zienkiewicz, O. C., & Taylor, R. L., The finite element method: Volume 2, solid mechanics (5th ed.). Butterworth-Heinemann.
19. J.N. Reddy, An introduction to nonlinear finite element analysis, Oxford University press,2004
20. Jean-Louis Batoz, Gouri Dhatt, Incremental displacement algorithms for non-linear problems, John Wiley & Sons, Ltd,1979
21. Ramm, E. (1981). Strategies for Tracing the Nonlinear Response Near Limit Points. In: Wunderlich, W., Stein, E., Bathe, KJ. (eds) Nonlinear Finite Element Analysis in Structural Mechanics. Springer, Berlin, Heidelberg. https://doi.org/10.1007/978-3-642-81589-8_5
22. IRC:5-2015: Standard specifications and code of practice for road bridges, section-I, general features of design (eighth revision), Indian Roads Congress
23. IRC:112-2020: Code of practice for concrete road bridges (first revision), Indian Roads Congress.
24. Darwin D, Pecknold D.A. Analysis of cyclic loading of plane r/c structures, computers & structures, vol.7, p.p 137-147, Pergamon Press Ltd.,1977.
25. Helmut Kupfer, Hubbert, Harsdorf, Behavior of concrete under biaxial stresses, ACI journal, August, 1969.
26. Wang. W.Y., Nonlinear hypo elastic analysis of reinforced concrete flat plate floors, Ph.D. thesis, Nanyang Technological University, Singapore, 2007
27. Ganaba, T. H. (1985). Nonlinear finite element analysis of plates and slabs (Doctoral dissertation, University of Warwick). Warwick Research Archive Portal (WRAP). warwick.ac.uk
28. He, Xiaogang, constitutive modeling of reinforced concrete for nonlinear finite element analysis, Ph.D. Thesis, The University of Hong Kong, 1999
29. H.T. Hu and W.C. Schnobrich, Nonlinear finite element analysis of reinforced concrete plated and shells under monotonic loading, Computers Structures, Vol.38, No.5/6, p.p 637-651, 1991
30. W.F. Chen, H. Suzuki, Constitutive models for concrete, computers & structures, vol.12, p.p 23-32, Pergamon Press Ltd.,1980.
31. Zhenhai Guo, Principals of reinforced concrete, first edition 2014, Butterworth-Heinemann publications
32. M. Ebrahim Tasuji, Arthur. H. Nilson, and Floyd. O. Slate, Biaxial stress-strain relationships for concrete, Magazine of Concrete Research: Vol. 31, No. 109: December 1979.